Growth and Properties of LiGaX2 (X: S, Se, Te) Single Crystals for Nonlinear Optical Applications in the Mid-IR

Article *in* Crystal Research and Technology · July 2003

DOI: 10.1002/crat.200310047

CITATIONS
95

READS
250

10 authors, including:

L. I. Isaenko
Sobolev Institute of Geology and Mineralogy
282 PUBLICATIONS **2,612** CITATIONS
SEE PROFILE

Valentin Petrov
Max Born Institute for Nonlinear Optics and S…
728 PUBLICATIONS **8,374** CITATIONS
SEE PROFILE

Jean-Jacques Zondy
Nazarbayev University
176 PUBLICATIONS **2,599** CITATIONS
SEE PROFILE

Vitaliy Vedenyapin
Sobolev Institute of Geology and Mineralogy
20 PUBLICATIONS **293** CITATIONS
SEE PROFILE

Cryst. Res. Technol. **38**, No. 3 – 5, 379 – 387 (2003) / **DOI** 10.1002/crat.200310047

Growth and properties of $LiGaX_2$ (X = S, Se, Te) single crystals for nonlinear optical applications in the mid-IR

L. Isaenko[1], A. Yelisseyev*[1], S. Lobanov[1], A. Titov[1], V. Petrov[2], J.-J.Zondy[3], P. Krinitsin[1], A. Merkulov[1], V. Vedenyapin[1], J. Smirnova[1]

[1] Design & Technological Institute of Monocrystals, 43 Russkaya str., Novosibirsk 630058, Russia
[2] Max-Born-Institute for Nonlinear Optics and Ultrafast Spectroscopy, 2A Max-Born-Strasse, D-12489 Berlin, Germany
[3] BNM-LPTF, Observatory of Paris, 61 Av. de l'Observatoire, F-75014 Paris, France

Received 14 October 2002, accepted 17 December 2002
Published online 15 April 2003

Key words crystal growth, light absorption, refractive indices, phase-matching, Li-containing ternary compounds.
PACS 42.70.Mp, 78.20.Ci

Single crystals $LiGaX_2$ (X = S, Se, Te) of optical quality were grown, with transparency ranges at 5 cm^{-1} absorption level of 0.32-11.6 μm, 0.37-13.2 μm and 0.54-14.2 μm, respectively. The first two, $LiGaS_2$ and $LiGaSe_2$, have a wurtzite-type structure whereas $LiGaTe_2$ is tetragonal (chalcopyrite lattice). The three refractive indices were measured in the whole transparency ranges of $LiGaS_2$ and $LiGaSe_2$ and n_a and n_c were found to be very close (quasi-uniaxial optical anisotropy) with a crosspoint at 6.5 μm ($LiGaS_2$) and 8 μm ($LiGaSe_2$). Sellmeier equations were fitted and phase-matching conditions for second harmonic generation (SHG) were calculated: the 1.467-11.72 μm spectral range for the fundamental is covered by $LiGaS_2$ and $LiGaSe_2$.

1 Introduction

Recently two lithium-containing nonlinear optical crystals, $LiInS_2$ (LIS) and $LiInSe_2$ (LISe), were successfully grown with high optical quality and applied for second harmonic generation (SHG) and optical parametric amplification (OPA) in the mid-IR [1, 2]. Their nonlinear susceptibilities and transparency ranges were found similar to those of the well-known $AgGaS_2$ but a number of additional advantages related to the wurtzite-type structure, the larger band gap and the higher thermal conductivity are very promising and stimulate the further search for new representatives of this family of synthetic crystals. In the present paper we report the growth of three new Li-containing ternary compounds with optical quality, $LiGaS_2$ (LGS), $LiGaSe_2$ (LGSe) and $LiGaTe_2$ (LGT) single crystals, and the results concerning their structure and linear optical properties. Of these only LGS and LGSe have been previously synthesized [3-6] but optical properties reported include only the band gaps [5-6]. LGS and LGSe were found in the present work to have the same wurtzite-type structure like LIS and LISe whereas LGT has a chalcopyrite lattice. All the three crystals reported are noncentrosymmetric: they possess the essential property of a nonzero second order nonlinear susceptibility $\chi^{(2)}$. The new crystals are transparent in a wide spectral range from the UV-visible to the mid-IR. The IR cut-off is determined by Li-X vibrations and shifts by about 2 μm to longer wavelengths in the S→Se→Te series. The three refractive indices of LGS and LGSe were measured in the present work and it is shown that the birefringence is sufficient for phase-matched nonlinear three wave interactions. SHG phase-matching curves are presented for propagation in the principal planes.

* Corresponding author: e-mail: elis@mail.nsk.ru

2 Experimental

Single crystals of $LiGaX_2$ (X=S, Se, Te) were grown using the Bridgman-Stockbarger technique. These compounds were synthesized from elementary Ga, S, Se and Te of 99.999% purity and Li of 99.9 %, which had been additionally purified using distillation and directed crystallization processes. To avoid atmospheric influence the components weighing and their mounting inside the reactor were performed in a chamber filled with an inert gas. The crystals were grown on a seed oriented along the [001] direction in a glasscarbon crucible located inside a silica ampoule. The ampoule was shifted from the hot zone to the cold one with 0.1 to 1 mm/h rate. Deviations from stoichiometric composition in the as-grown crystals result in colour changes and/or turbidity as in the case of LIS [7]. These properties were controlled using high-temperature after-growth annealing. In this case a source with the component, in which the as-grown crystal was found deficient, was placed into a silica ampoule together with the crystal. The ampoule was heated then up to a temperature, which was several degrees below the crystal melting point for a period of up to several days, depending on crystal/boule size.

The crystal structure of LGS and LGSe was determined by an Enraf-Nonius CAD-4 [8] diffractometer using the SHELX-97 [9] structure refinement program. For LGT powder X-ray diffraction was studied by a Philips PW1700 diffractometer and the PCW2.3 program [10] was used for cell parameter determination.

Transmission spectra in the UV-visible and near-IR spectral ranges were recorded using a MDR2 grating monochromator equipped with a 30 W incandescent lamp and FEU100 or FEU62 photomutipliers as detectors. The transmission in the mid-IR spectral range was measured by a Bomem FTIR spectrometer. Raman spectra in the backscattering were recorded using a Renishaw Ramascope Blue 488 with a CCD camera. The absorption coefficients were determined from the experimentally measured transmission spectra taking into account the Fresnel reflections at normal incidence.

The refractive indices versus wavelength were measured in the transparency range of LGS and LGSe by the technique of minimum deviation angle. A beam from D_2, incandescent lamps or from a globar was used for this purpose after passing through a SPM2 prism monochromator for wavelength selection. The prism manufactured from the crystal under investigation was located on the axis of a G5 goniometer. A combination of photomultipliers, photodiodes and a cooled MCT detector allowed us to cover the spectral range from the UV to the mid-IR. The beam-shaping optics in our set-up contained only reflective elements (systems of cylindrical concave mirrors) in order to minimize the wavelength dependence. The desired polarization was selected using a set of film or grid polarizers. Only LGS and LGSe were available in sufficient size and quality for this measurement: two prisms with different orientation and optically polished faces were manufactured from each of these crystals. Characteristic dimensions (height and edges) were 8.5 and 5.5 mm for LGS and LGSe, respectively. The accuracy of orientation was ~0.3°. The apex angles of the prisms were 33.05 and 33.9° for LGS and LGSe, respectively. The apex angle was chosen to optimize the precision of index measurement assuming a nominal index equal to 2.3. The three refractive indices were measured with an accuracy of ±0.0001.

3 Results and discussion

3.1 $LiGaX_2$ single crystals

Single crystals of LGS and LGSe, up to 15 mm in diameter and 40 mm long, of sufficient optical quality were grown as can be seen in Fig. 1. Up to now only small LGT samples of dimensions not larger than several millimeters could be obtained. LGS is almost colourless with a slight rose tint whereas LGSe is yellow-greenish. The quality of the LGSe samples was better; more inclusions can be observed in LGS (Fig. 1). The crystallization temperature is 1040, 850 and 600°C for LGS, LGSe and LGT, respectively. The lower crystallization temperature of LGSe is supposed to be the reason for its higher optical quality as compared to LGS. For each crystal the colour varies from sample to sample depending on the composition, as observed for LIS [7]. For LGS it changes from colourless to reddish, for LGSe from yellowish to dark red while for LGT from orange to black (opaque in the visible region).

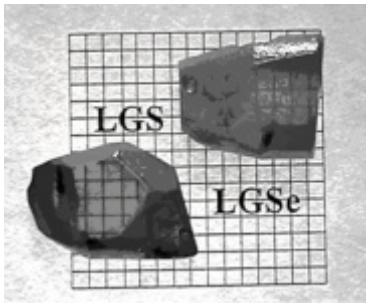

Fig. 1 Fragments of single crystal boules of $LiGaS_2$ (above) and $LiGaSe_2$ (below) with polished opposite faces. A grid beneath the samples with 2 x 2 mm^2 cells serves to show the scale.

Table 1 Crystallographic parameters.

Formula	$LiGaS_2$ Present paper	[4]	$LiGaSe_2$ Present paper	[5]	$LiGaTe_2$
formula wt	140.78	140.78	234.58	234.58	321.86
crystal system	orthorhombic	orthorhombic	orthorhombic	orthorhombic	tetragonal
a (Å)	6.5133(6)	6.519(6)	6.832(1)	6.833	6.338
b (Å)	7.8629(8)	7.872(7)	8.237(1)	8.227	6.338
c (Å)	6.2175(5)	6.238(4)	6.535(1)	6.541	11.704
V (Å ^{3})	318.45(5)	320.1	367.7(1)	367.7	470.1
Z	4	4	4	4	16
space group	$Pna2_1$	$Pna2_1$	$Pna2_1$	$Pna2_1$	$I\bar{4}2d$
T (K)	296	293	293	293	295
diffractometer	Enraf-Nonius CAD4		Enraf-Nonius CAD4		Philips PW1700
λ(Å)	0.71073 (Mo Kα)	0.71073	0.71073		1.54060 (Cu Kα)
ρ_{calc} (g/cm^3)	2.937	2.92	4.237		4.689
2θ range	8.12 to 70.0°		7.76 to 70.0°		
total data	863		977		
obsd data[a]	809		857		
refinement method	SHELXL-97		SHELXL-97		PCW2.3
R $(F)^b_{tot}$	0.0297	0.049	0.0523		
R $(F)_{obs}$	0.0279		0.0468		
wR$(F^2)^c_{tot}$	0.0768		0.1306		
wR$(F^2)_{obs}$	0.0752		0.1248		

[a] –I > 2σ(I). [b] – $R = \Sigma||F_o| - |F_c||/ \Sigma|F_o|$. [c] - $wR = [\Sigma w(|F_o| - |F_c|)^2/ \Sigma w|F_o|^2]^{1/2}$.

3.2 Crystal structure

For LGS and LGSe the results of the single-crystal X-ray analysis are given in Tables 1 and 2 and for comparison the crystal X-ray results on LGS from [4] and the powder X-ray results for LGSe from [5] are also included. For the first time to our knowledge we present here single crystal X-ray analysis of LGSe and powder X-ray analysis of LGT. LGS and LGSe were found to have the orthorhombic structure with $Pna2_1$ space group (mm2 point group) and are thus isostructural to LIS and LISe, whereas LGT is tetragonal ($I\bar{4}2d$ space group and $\bar{4}2m$ point group) and thus isostructural to $LiInTe_2$ [11].

All structures are characterized by a dense packing of atoms with tetrahedral and octahedral cavities. One half of the tetrahedron cavities are occupied by Li^+ and Ga^{3+} cations, while the other half of the tetracavities and all octacavities are empty. The difference between orthorhombic and tetrahedral structures is due to the different way of their packing. The main feature of the orthorhombic structure is a hexagonal anion packing, whereas the tetragonal structure has a face-centered cubic packing for the anion sublattice. In the orthorhombic

structure each MX_4 tetrahedron has three common faces with empty tetrahedron cavities and one common face with an empty octahedron cavity. In the tetragonal structure each MTe_4 tetrahedron has two common faces with tetra- and octacavities. As a result, one can expect a higher cation mobility and a larger amount of point defects in the tetragonal structure in comparison to the orthorhombic one. The lattice parameters were only weakly dependent on crystal colour for each of the $LiGaX_2$ crystals examined.

Table 2 Atomic positional parameters.

atom	X	Y	Z	U_{eq} [a]
		$LiGaS_2$		
Ga	0.07347(4)	0.87402(4)	0.62281(6)	0.0101(1)
Li	0.417(1)	0.877(1)	0.116(4)	0.015(3)
S(1)	-0.0944(1)	0.6367(1)	0.5080(2)	0.0117(3)
S(2)	0.0662(1)	0.8836(1)	0.9894(2)	0.0118(3)
		$LiGaS_2$ [4]		
Ga	0.0736(3)	0.8729(4)	0.6135	
Li	0.418(5)	0.855(5)	0.126(2)	
S(1)	-0.0951(6)	0.635(1)	0.6065(8)	
S(2)	0.0659(7)	0.885(1)	0.988(1)	
		$LiGaSe_2$		
Ga	0.0730(1)	0.8741(1)	0.6229(2)	0.0129(2)
Li	0.410(3)	0.878(1)	0.118(8)	0.029(6)
Se(1)	-0.0936(1)	0.6348(1)	0.5064(2)	0.0144(2)
Se(2)	0.0661(1)	0.8814(1)	0.9907(2)	0.0144(2)

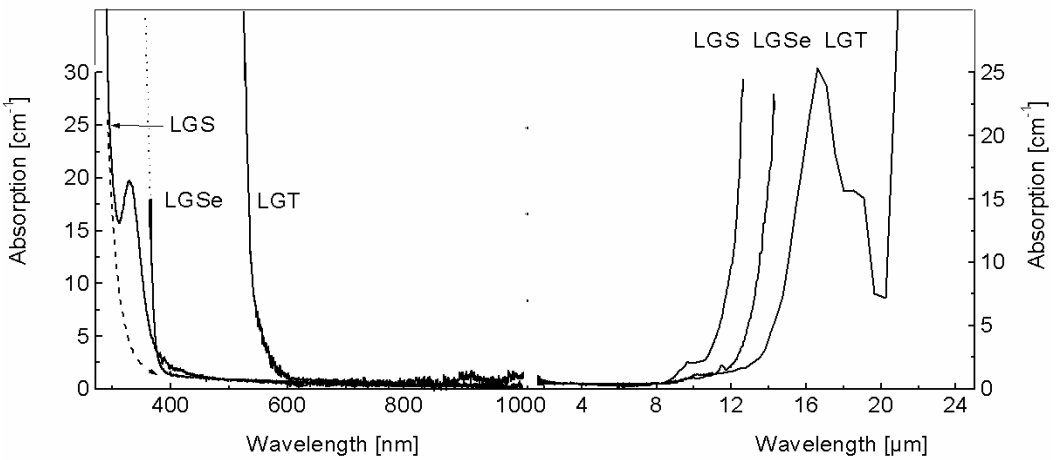

Fig. 2 Absorption spectra of LGS, LGSe and LGT single crystals at 300 K.

3. 3 Optical spectroscopy

The unpolarized absorption spectra recorded for $LiGaX_2$ crystals, about 1 mm thick, are shown in Fig. 2. These spectra correspond to almost colourless LGS, slightly yellowish LGSe and red LGT samples. In the spectrum for LGS one can see an intense broad band with a maximum at 330 nm near the fundamental absorption edge, as previously observed for LIS [7]. The transparency ranges at a level of 5 cm^{-1} are 0.32-11.6 μm (after substraction of the 330 nm near-edge band), 0.37-13.2 μm and 0.54-14.2 μm for LGS, LGSe and LGT, respectively. A well-pronounced maximum at 16 μm with a shoulder at ~18 μm can be seen in the absorption spectrum for LGT: further increase of the absorption takes place at 20 μm. Extrapolating the linear part of the

$(\alpha h\nu)^2$ dependence versus the photon energy $E = h\nu$ (the case of allowed direct transitions between valence and conduction bands [12]) we estimated the band gap energies: E_g= 4.15 eV (LGS), 3.34 eV (LGSe) and 2.3 eV (LGT) at room temperature. The former two values are higher than those given in Ref. [6]: 3.62 and 3.13 eV for LGS and LGSe, respectively. The band gap for LGT is much larger in comparison to tellurides containing other cations. For example, for $AgGaTe_2$ it is only 1.316 eV [13].

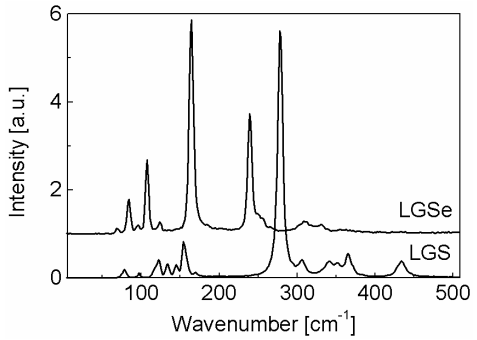

Fig. 3 Raman spectra of LGS and LGSe single crystals recorded with 488 nm Ar^+ laser excitation at 300 K.

The Raman spectra recorded for LGS and LGSe are presented in Fig. 3. The group analysis shows that, at the zone centre for this structure, the 48 normal modes are distributed among the various irreducible representations of the C_{2V} factor group as follows:

$$G^{vib} = 12A_1 + 12A_2 + 12B_1 + 12B_2 \tag{1}$$

The acoustic modes have A_1, B_1 and B_2 symmetries; the remaining 45 (optical) modes are Raman-active. Detailed analysis of the Raman spectra and comparison with IR reflectivity spectra [6] allowed to separate two groups of vibrations, which are located for LGS at 250 to 450 cm^{-1} with a dominating line at 280 cm^{-1}, and below 200 cm^{-1}. They are related to Li-S and Ga-S vibrations, respectively [6]. The low-frequency modes are highly covalent whereas the high-frequency modes are mainly ionic [6]. For LGSe these groups shift to 60-130 cm^{-1} and 150-350 cm^{-1} (with a dominating line at 166 cm^{-1}), respectively. The change in the energy for vibrations with chalcogen participation when replacing S by Se is in a good agreement with estimations based on changes in the ion masses M. The ratio between the experimentally measured phonon energies in the most intense line is $h\nu(S)/h\nu(Se)$ = 1.68 and the expected value is $(M_{Se}/M_S)^{1/2}$ = 1.87. The corresponding shift in the long-wave transparency edge shows that the mid-IR cut-off is determined by a two-phonon absorption process.

3.4 Index of refraction and phase-matching conditions

Refractive indices for LGS and LGSe were measured as function of wavelength λ in the whole transparency range and the results are plotted in Fig. 4. The principal values n_a and n_c appear to be very close and there is a crosspoint between them at ~6.5 μm for LGS and at ~ 8 μm for LGSe. Thus with the convention $n_x < n_y < n_z$ the correspondence between the principal optical and the crystallographic axes is $xyz \Leftrightarrow bac$ up to these crosspoints while $xyz \Leftrightarrow bca$ holds at λ > 6.5 μm (LGS) and at λ > 8 μm (LGSe). The birefringence $(n_c - n_b)$ and $(n_a - n_b)$ (Fig. 5) amounts to ~0.04 for LGS and ~0.05 for LGSe. This is comparable with that of $AgGaS_2$ (~0.05), LIS (~0.04) and LISe (0.046). Thus LGS and LGSe are expected to be broadly phase-matchable. The angle $2V_z$ between the two optical axes of these biaxial crystals varies from 138° (148°) to 180° for LGS (LGSe), where the maximum $2V_z$ = 180° corresponds to the crosspoints between n_a and n_c. Both LGS and LGSe are thus optically negative biaxial crystals. Both can be regarded as quasi-uniaxial and in

the crosspoints they become uniaxial. The principal values of the refractive indices were fitted by Sellmeier equations of the type:

$$n_i^2 = A_i + B_i \Big/ \left(l^2 - C_i \right) - D_i l^2 , \tag{2}$$

where $i = x, y, z = b, a, c$; λ the wavelength in μm and the coefficients A_i, B_i, C_i and D_i given in Table 3.

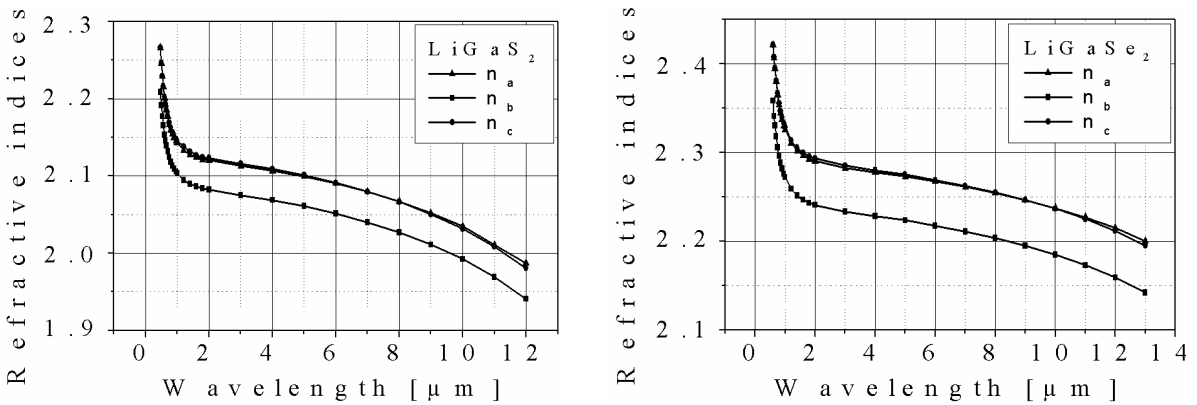

Fig. 4 Refractive indices versus wavelength for (a) LGS and (b) LGSe at 300 K.

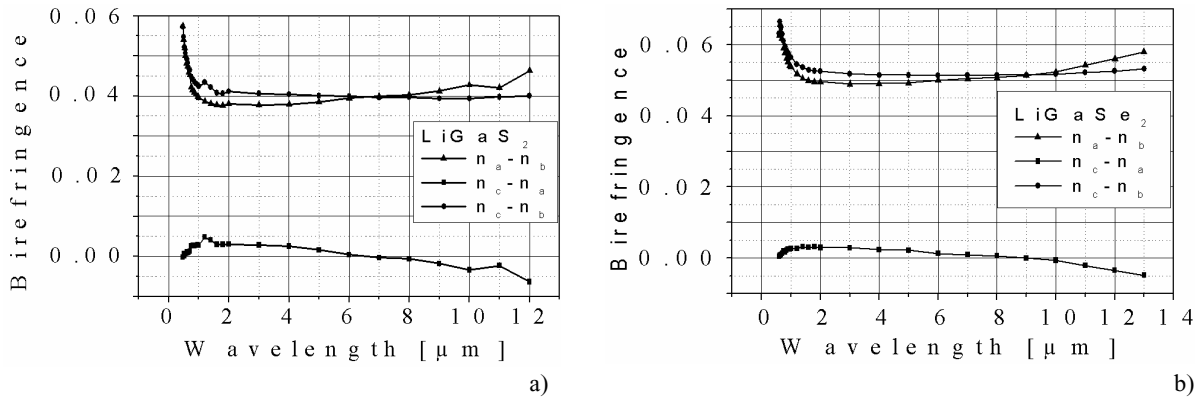

Fig. 5 Birefringence in (a) LGS and (b) LGSe single crystals as a function of wavelength λ.

Table 3 The Sellmeier coefficients for LGS and LGSe.

Coefficient	$LiGaS_2$	$LiGaSe_2$
A_x	4.326834	4.99592
B_x	0.1030907	0.1513
C_x	0.0309876	0.08989
D_x	0.0037015	0.00233
A_y	4.478907	5.20896
B_y	0.120426	0.18632
C_y	0.034616	0.07687
D_y	0.0035119	0.00211
A_z	4.493881	5.22442
B_z	0.1177452	0.18365
C_z	0.0337004	0.07493
D_z	0.0037767	0.00232

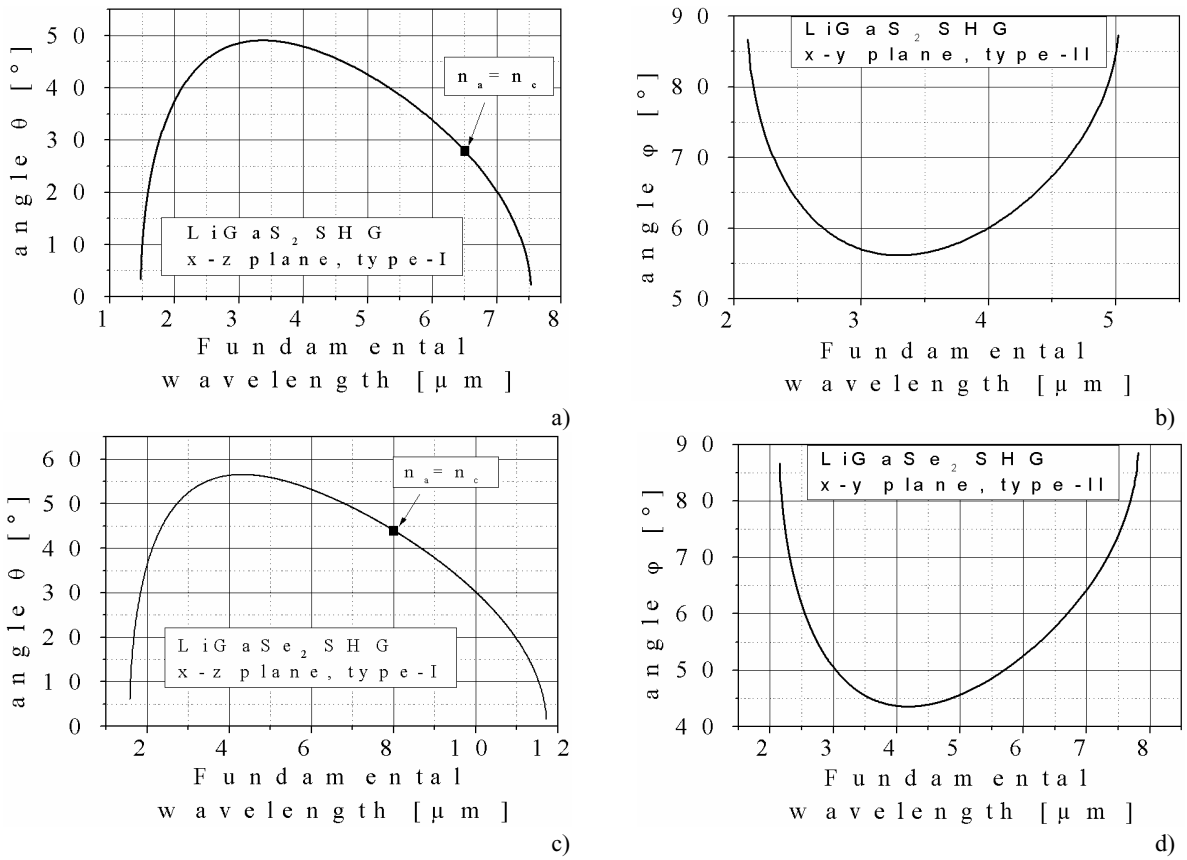

Fig. 6 Phase-matching angles versus fundamental wavelength for SHG in (a, b) LGS and (c, d) LGSe in the (a, c) *x-z* and (b, d) *x-y* planes. The black squares in a and c indicate the points where $n_a=n_c$.

The expressions for the effective second order nonlinearity d_{eff} correspondence between the crystallographic and the principal optical axes because the nonlinear coefficients are for nonlinear crystals of the mm2 crystallographic class, which are given in the *xyz* system, depend on the chosen defined traditionally in the *abc* system. For that purpose an unique choice is preferable and we established that, with the assumption *xyz* ⇔ *bac* (as already mentioned above), the corresponding expressions in the principal planes:

$$x-y: \qquad d_{eff}^{eoe} = d_{eff}^{oee} = d_{24}\sin^2 j + d_{15}\cos^2 j, \tag{3a}$$

$$y-z: \qquad d_{eff}^{oeo} = d_{eff}^{eoo} = d_{24}\sin q, \tag{3b}$$

$$x-z, q < V_z: \qquad d_{eff}^{ooe} = d_{31}\sin q, \tag{3c}$$

$$x-z, q > V_z: \qquad d_{eff}^{oeo} = d_{eff}^{eoo} = d_{15}\sin q, \tag{3d}$$

remain unaffected by the crosspoints of n_a and n_c. This is so because phase-matching can be achieved only for propagation directions away from the two optical axes, V_z is close to 90°, and in practice Eq. (3d) is never realized (see Fig. 6a, c). In equations (3) the q and j angles determine direction of a light beam propagation

inside crystal in polar coordinates. The upper index at *d* shows the type of interaction [14] and the lower one indicates the component of *d* tensor. From Eqs. (3) it is clear that LGS and LGSe behave as optically negative uniaxial crystals in the *x*-*y* plane (type-II interaction), as optically positive in the *y*-*z* plane (type-II interaction) and as optically negative (type-I interaction) or positive (type-II interaction) in the *x*-*z* plane. Under Kleinmann symmetry $d_{31}=d_{15}$ holds [14].

Table 4 The fundamental wavelength ranges in μm for SHG in LGS, LGSe, LIS, and LISe.

Plane/Crystal	LGS	LGSe	LIS	LISe
x-y, type-II, eoe	2.105 – 5.026	2.146 – 7.812	2.30 – 5.79	2.73 – 8.24
x-z, type-I, ooe	1.467 – 7.536	1.571 – 11.72	1.74 – 7.93	2.08 – 12.4
y-z, type-II, oeo	2.105 – 2.301	2.146 – 2.217	2.30 – 2.65	2.73 – 3.07
y-z, type-II, oeo	4.838 – 5.026	7.759 – 7.812	5.09 – 5.79	7.66 – 8.24

Fig. 6 shows the calculated SHG phase-matching curves for LGS and LGSe in the *x*-*y* and *x*-*z* principal planes (in the *y*-*z* plane the tuning is very limited). In Table 4 the calculated SHG ranges for the fundamental wavelength are given for LGS and LGSe, and also for LIS and LISe for comparison. One can see that the short-wave limits for the fundamental wavelength are shifted to shorter values in the Ga-containing compounds as compared to the In-containing compounds. Thus SHG below 1.5 μm is already possible with LGS whereas the lower limit for LIS is ~ 1.7 μm. Since $\chi^{(2)}$ correlates with the band gap, similar nonlinearities are expected for LGS and LGSe, as those determined for LIS and LISe [1,2]. Work is in progress to estimate the nonlinear coefficients from phase-matched SHG measurements.

4 Summary

The fundamental structural and optical properties of $LiGaX_2$ (X = S, Se, Te) single crystals are reported. These properties include lattice parameters, index of refraction, birefringence, transmission/absorption spectra in the transparency range and band gap values. The lattice structure was found to be of wurtzite type for X = S, Se and of chalcopyrite type for X = Te. The average index for the IR region was found to be 2.1 and 2.25 for LGS and LGSe, respectively. The corresponding band gap values are 4.15 (LGS), 3.34 (LGSe) and 2.3 eV (LGT). The value E_g = 4.15 eV for LGS is the largest among all known ternary chalcogenides used for nonlinear optical applications in the mid-IR: therefore LGS based OPA can be pumped near 800 nm without the onset of two-photon absorption as demonstrated with LIS [1]. The position of the IR cut-off is determined by two-phonon processes: the maximum phonon energies are related to Li-X vibrations. Both the *a* and *c* lattice parameters and the n_a and n_c refractive indices are very close which allows us to classify LGS and LGSe as quasi-tetragonal and quasi-uniaxial crystals. The $n_a(l)$ and $n_c(l)$ curves exhibit crosspoints at 6.5 and 8 μm for LGS and LGSe, respectively. Sellmeier equations were constructed and the phase-matching conditions calculated for SHG. LGS and LGSe crystals were found to be phase-matchable for SHG for fundamental wavelengths extending from 1.467 to 11.72 μm.

Acknowledgements This work was partly supported by the European Community INCO-COPERNICUS program (grant No ERBIC15-CT98 0814) and CRDF (grant RE2-2222 proposal 6410).

References

[1] L. Isaenko, A. Yelisseyev, S. Lobanov, V. Petrov, F. Rotermund, J.-J. Zondy, G. H. M. Knippels, Mater. Sci. Semicond. Processing **4,** 665 (2001).

[2] L. Isaenko, A. Yelisseyev, S. Lobanov, V. Petrov, F. Rotermund, G. Slekys, J.-J. Zondy, J. Appl. Phys. **91,** 9475 (2002).

[3] Z.Z. Kish, V. V. Loshchak, E.Yu. Peresh, E.E. Semrad, Inorg. Mater. **25,** 1658 (1989), [translated from Izvestiya Akademii Nauk SSSR: Neorganicheskie Materialy **25,** 1959 (1989)].

[4] J. Leal-Gonzalez, S.S. Melibary, A.J. Smith, Acta Cryst. C **46,** 2017 (1990).
[5] K. Kuriyama, T. Nozaki, J. Appl. Phys. **52,** 6441 (1981).
[6] A. Eifler, V. Riede, J. Brückner, S. Weise, V. Krämer, G. Lippold, W. Schmitz, K. Bente, W. Grill, Jpn. J. Appl. Phys. **39** (Suppl. 39-1) 279 (2000).
[7] L. Isaenko, I. Vasilyeva, A. Yelisseyev, S. Lobanov, V. Malakhov, L. Dovlitova, J-J. Zondy, I. Kavun, J. Cryst. Growth **218,** 313 (2000).
[8] Enraf-Nonius, CAD-4 Software. CD4CAO (Version 5.0), CADDAT (Version 5.1), Enfar-Nonius, Delft, The Netherlands (1989).
[9] G. M. Sheldrick, SHELXS97 and SHELXL97, University of Goettingen, Germany (1997).
[10] W. Kraus, G. Nolze, PowderCell for Windows, Version 2.3. BAM, Berlin, Germany (1999).
[11] G. Kühn, E. Pirl, H. Neumann, E. Nowak, Cryst. Res. Technol. **22,** 265 (1987).
[12] J.I. Pankove, Optical proceses in semiconductors (Prentice-Hall Englewood Cliffs, New Jersey, 1971), p. 456.
[13] M. C. Ohmer, J. T. Goldstein, D. E. Zelmon, A. W. Saxler, S. M. Hedge, J. D. Wolf, P. G. Schunemann, T. M. Pollak, J. Appl. Phys. **86,** 94 (1999).
[14] V. G. Dmitriev, G. G. Gurzadyan, D. N. Nikogosyan, Handbook of nonlinear optical crystals, Springer, Berlin 1997, p.29.